

## Sloshing reduction effect of splitting wall in cylindrical tank

D.Takabatake<sup>1</sup>, S.Sawada<sup>2</sup>, N.Yoneyama<sup>2</sup> and M.Miura<sup>3</sup>

<sup>1</sup> Central Research Institute of Electric Power Industry, 1646, Abiko, Abiko, Chiba, Japan

<sup>2</sup> Professor, Disaster Prevention Research Institute, Kyoto University, Gokasho, Uji, Kyoto, Japan

<sup>3</sup> Idemitsu Engineering Co., Ltd, Mihama, Chiba, Japan

Email: tdaisuke@criepi.denken.or.jp, sawada@catfish.dpri.kyoto-u.ac.jp, yoneyama@taisui5.dpri.kyoto-u.ac.jp, miura@catfish.dpri.kyoto-u.ac.jp

### ABSTRACT :

Many petroleum tanks were damaged by sloshing during 2003 Tokachi-oki, Japan. Large earthquakes are predicted to occur within 50 years, which will cause the similar damage. In this paper, we develop a splitting wall as a new sloshing reduction device. Model experiments and numerical simulations are performed to examine the effect of the device. The experimental results indicate the proposed device is effective to reduce sloshing against sinusoidal input motion. We also perform numerical study to simulate the experimental result. Both experimental and numerical results are almost same. Based on the numerical simulation, the proposed device can be also effective against earthquake ground motion.

### KEYWORDS:

sloshing, splitting wall, reduction of sloshing

### 1. INTRODUCTION

The liquid sloshing is free-surface fluctuation of liquid when its container is excited by external vibrations such as earthquakes. The liquid sloshing may cause various engineering problem, for example instability of ships in aero engineering and ocean engineering, failures on structural systems of the liquid container.

During 1964 Alaska earthquake, many tanks suffered typical damage such as fire, buckling of floating roofs, caving of fixed roofs and failures on structural systems on tanks, even if its location is about 150 km far from the epicenter. In Japan, many petroleum tanks were damaged by the sloshing during 1964 Niigata earthquake, 1983 Nihonkai-chubu earthquake and 2003 Tokachi-oki earthquake. During 2007 Chuetsu-oki earthquake, radiation-contaminated water in a nuclear power plant spilled. The sloshing is caused by long period seismic motion and may give damages in large area even if its location is far from the epicenter.

In Japan, large earthquakes, such as Tokai, Tonankai, and Nankai earthquakes, are predicted to occur within 50 years, which will give the similar damage to the existing tanks. Development of sloshing reduction device is expected and experimental, analytical and numerical approaches are done now.

One of the examples of the device is annular ring baffles, whose shape is like a disc, installed below the liquid surface. J.R.Cho and S.Y.Lee examined the effect of the baffles, which suppress the flow motion, by varying the number of baffles, the distance from the free surface and the inner-hole diameter. They used the finite element method for modeling the structural motion and the interior liquid flow assuming interior liquid incompressible. They concluded that the best damping effect is achieved when the inner-diameter of the baffle is half of the diameter of tank and baffle is located at 65-75% of the fill height of interior liquid.

We propose the splitting wall as sloshing reduction device. The splitting wall installed in tanks vertically, which consists of solid panels with slits, gives resistance to liquid moving. In order to examine effects of the splitting wall we conduct model experiments and perform numerical simulations on the model scale and real scale. The model used in experiments is cylindrical tank whose diameter is 512 mm. 21 cases of the shaking table tests are carried out varying the layout of splitting wall using sinusoidal input motion with wide variety frequency. Based on the result we propose the most effective splitting wall which can reduce both sloshing height and fluid load acting on the splitting wall for wide frequency range. We also perform the three dimensional incompressible fluid analysis using finite difference method to simulate model experiments. For tracing free-surface of liquid, Volume Of Fluid (VOF) method is used. The results show the numerical method used can accurately simulate sloshing behaviors in cylindrical tank with the splitting wall. We finally calculate the sloshing response against the observed ground motion recorded during 2003 Tokachi-oki earthquake. The result indicates that the proposed splitting wall is also effective to reduce sloshing against seismic motion.

## 2. MODEL EXPERIMENT

### 2.1. Experimental Condition



Fig.1 Experimental set up

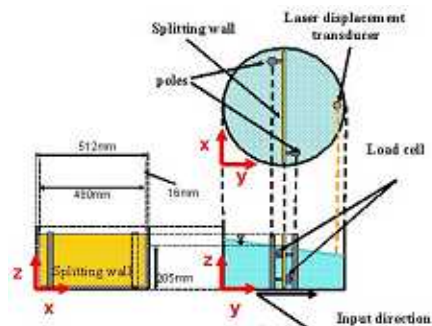


Fig.2 Model of tank

We perform shaking table experiments the model scale to examine the effect of the splitting wall. Experimental set up is showed in Fig.1 and Fig.2. The tank model, whose diameter is 512 mm, height 390 mm, liquid depth 205 mm, is made of acrylic resin. Note that it is stiff enough to ignore the deformation of tank walls.

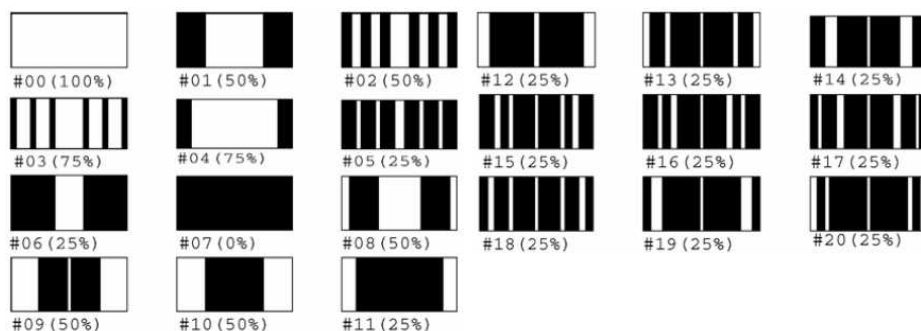


Fig.3 Slit layout of splitting walls

(Black shows the panel and white shows opening are).

Tab.1 Slit parameters of splitting walls

case	opening ratio	number of opening area			
#00	100%	1	#11	25%	2
#01	50%	1	#12	25%	3
#02	50%	5	#13	25%	3
#03	75%	5	#14	25%	5
#04	75%	1	#15	25%	5
#05	25%	5	#16	25%	5
#06	25%	1	#17	25%	5
#07	0%	0	#18	25%	5
#08	50%	3	#19	25%	3
#09	50%	3	#20	25%	5
#10	50%	2			

The splitting wall is made of a steel frame and brass panels whose heights are 240mm. The width of a steel frame is 480mm and there are two 16 mm gaps between tank wall and splitting wall. Six types of brass panels, whose widths are 20, 30, 40, 60, 90, 120 mm, are used. We can arrange variety of slit layout by selecting brass panels. 21 cases of layouts including no splitting wall case are examined, as shown in Fig.3 and Table 1. The opening ratio (OR), which is defined as the liquid passing area divided by whole section area on the splitting wall, is used as one of key parameters.

We set two poles, whose diameter is 20mm, standing on the bottom of tank as shown in Fig.2 to support the splitting wall with four rubber joints. Two of the four joints have load cells to measure the fluid load on the splitting wall, as shown in Fig.4. The fluid load acting on the splitting wall is defined as twice the sum of forces measured by these load cells at left-down and right-up corners based on the symmetric condition.

The white-stained water, which makes possible to be measured its surface level by a laser displacement transducer, is used as interior liquid. Although the viscosity of white-stained water is different from that of

petroleum, we assume the difference very small and neglect it in the experiment.

Sinusoidal motion from 1.0 Hz to 3.0 Hz is input. If the sloshing height is large at 1.0 Hz or 3.0 Hz we expand the frequency range. Frequency increment is basically 0.1 Hz, while it is set to 0.01 Hz in the range the sloshing response is very large. The amplitude of sinusoidal input motion is set about 1 mm manually.

We discuss two parameters, one is a sloshing height beside tank wall measured by displacement transducer and the other is fluid load acting on the splitting wall by load cells described above. We also measure displacement of shaking table using a laser displacement transducer. We sample 3000 digital data at 200 Hz rate in 15 seconds, after sloshing motion become stable. The sloshing height is defined as half of difference between the maximum and minimum fluid surface levels in time history. We draw the sloshing amplitude response curve in which horizontal axis shows the frequency of sinusoidal input motion and vertical axis the normalized sloshing height by the amplitude of shaking table (about 1mm). We also show the response curve of fluid load acting on the splitting wall based on the same method, whose horizontal axis indicates the frequency and vertical axis the fluid load.

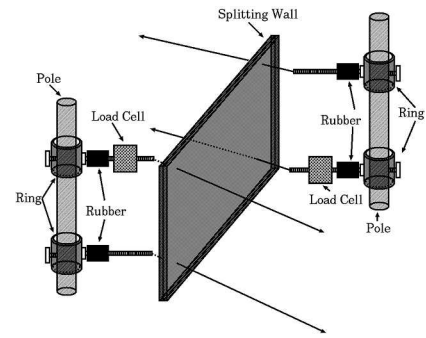


Fig.4 Setting the load cells

## 2.2 Experimental result

We compare the sloshing height and fluid load response curves to examine the effect of the splitting wall. Fig.5 shows the comparison of the sloshing height response curve between the no splitting wall case (OR=100% , case #00) and the full splitting case (OR=0%, case #07). In the case #00, two peaks appear on the response curve. The left peak is around 1.2 Hz that can be the first natural frequency, while another peak around 2.2 Hz the second natural frequency. The sloshing natural frequency without splitting wall is calculated by

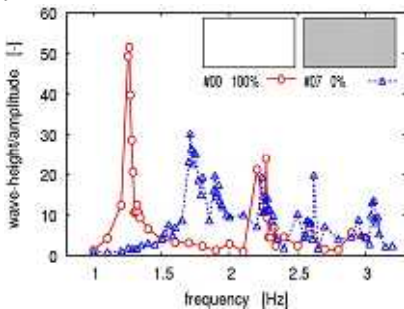


Fig.5 Comparison of sloshing height response curves between the cases #00( ) and #07( )

$$f_n = \frac{1}{T_n} = \frac{1}{2\pi \sqrt{\frac{R}{\epsilon_n g} \coth \frac{\epsilon_n H}{R}}} \quad (2.1)$$

where,  $f_n$  is  $n$ th natural frequency,  $T_n$   $n$ th natural period,  $R$  radius of tank,  $H$  liquid depth,  $\epsilon_n$   $n$ th positive root of Bessel function  $J_0(\epsilon)=0$ ,  $g$  gravity acceleration. The theoretical sloshing natural frequencies calculated from equation (2.1) are 1.26 Hz for the first mode and 2.20 Hz for the second mode, which are almost same as the experimental results. The sloshing natural frequency in the case with splitting wall cannot be calculated from equation (2.1). Fig.6 (a),(b)

show the free surface shapes of first and second natural sloshing modes obtained by numerical simulation (Numerical method is described later). Note that colors in the figure show velocity of interior liquid flow. The highest surface level is obtained at side end of the tank for first mode, while it is at the more central position for second mode. The sloshing height for first mode is larger than that for second mode.

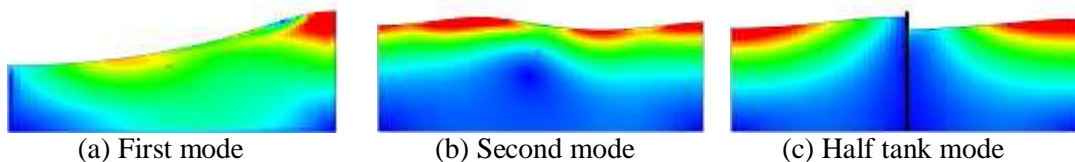
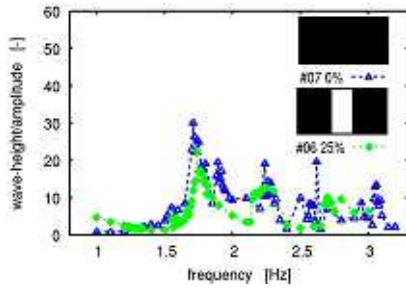
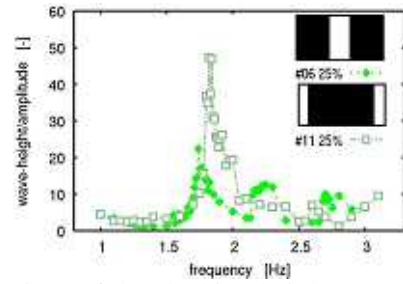


Fig.6 Shapes of free surface obtained by numerical simulation



**Fig.7** Comparison of the sloshing height response curves between the cases #07( ) and #06( )



**Fig.8** Comparison of the sloshing height response curves between the cases #06( ) and #11( )

We find two remarkable points in **Fig.5**; 1) response at first mode become smaller in the case #07 than that in the case #00, 2) new peak appears around 1.7Hz on response curve in the case #07. As the splitting wall divides the volume of the tank into two parts, the oscillatory system of the tank changes, that is, new natural frequencies are generated by the half volume of the tank. This peak appears in all cases with splitting wall. **Fig.6 (c)** shows the free surface shape of the new mode. This mode, which is generated for the half volume tank individually, is called as “half tank mode”.

We arrange various slit layouts on the splitting wall as shown in **Fig.3** (Case #07). **Fig.7** shows the comparison of the sloshing height response curve between the case #07 (OR=0%) and the case #06 in which the splitting wall opens at center (OR=25%). The peak value at half tank mode in the case #06 is smaller than that in the case #07.

To examine the effect of the slit position, two sloshing height response curves, whose cases have the same opening ratio 25%, are compared. **Fig.8** shows the comparison of sloshing height response curve between the case #06, in which the slit is located at center, and the case #11 with the slit at both side ends. The peak value at half tank mode in the case #11 is twice larger than that in the case #06. However the peak value at second mode in the case #06 is smaller than that in the case #11.

**Fig.9** shows the comparison of sloshing height response curves between the cases #11 and #12 to show the effect of narrow center slit, while the splitting walls in the cases have slits at both ends. The peak value at half tank mode in the case #12 is half of that in the case #11. This indicates that the cases with center slit give small sloshing height at half tank mode.

**Fig.10** shows the comparison of sloshing height response curve between in the cases #12 and #16. The splitting wall in the case 16 has single center slit and four narrow side slits as shown in **Fig.3**. While the peak value at first mode in the case #16 is slightly larger than that in the case #12, the peak value at half tank mode in the case #16 is much smaller than that in the case #12. **Fig.11** shows the comparison of sloshing height curves between the case #00, which is no splitting wall case, and the case #16. While the peak value at half tank mode in the case #16 is generated, the peak value at first mode in case #16 is one fifth of that in case #00 and the peak value at second mode in case #16 is half of that in case #00. Note that the sloshing height in the case #16 is small with wide frequency range. **Fig.12** also shows the comparison of the fluid load response curves between case #07, which is no slit case, and case #16. The fluid load in the case #16 is also small with wide frequency range.

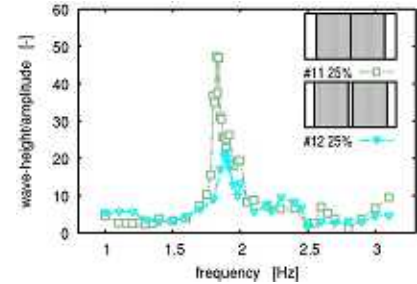


**Fig. 9** Comparison of sloshing height response curves between the cases #11( ) and #12( )

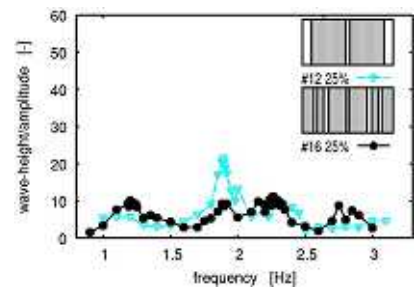


**Fig. 10** Comparison of sloshing height response curves between the cases #12( ) and #16( )

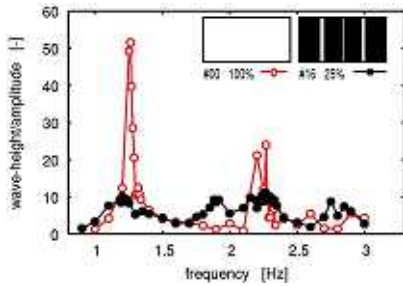


**Fig. 11** Comparison of the sloshing height response curves between the cases #00( ) and #16( )

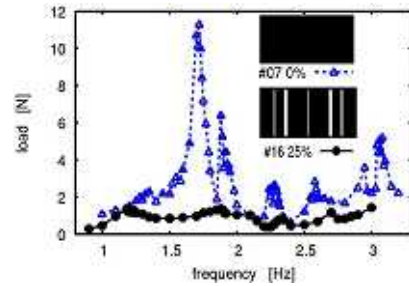


**Fig. 12** Comparison of the fluid load response curves between the cases #07( ) and #16( )

### 3. NUMERICAL SIMULATION

#### 3.1 Modeling

Our numerical simulation is based on the three-dimensional incompressible analysis method. When the density of fluid is assumed constant, the continuity equation and the momentum equation (Navier-Stokes equation) are described as:

$$\frac{\partial \bar{u}_i}{\partial x_i} = 0, \quad (3.1)$$

$$\frac{\partial u_i}{\partial t} + \frac{\partial u_i u_j}{\partial x_j} = G_i - \frac{1}{\rho} \frac{\partial p}{\partial x_i} + \frac{\partial}{\partial x_j} \left( \nu \frac{\partial u_i}{\partial x_j} \right), \quad (i=1,2,3) \quad (3.2)$$

where  $u_i$  is the velocity,  $G_i = (-\alpha, -\beta, -g)$  the external force on unit volume,  $p$  the pressure of fluid,  $\rho$  the density,  $\nu$  the constant which shows the kinematic viscosity of fluid,  $g$  the gravity acceleration,  $\alpha$  and  $\beta$  the input accelerations in the  $x$  and  $y$  directions, respectively. In this study, since the effect of the turbulent flow is assumed constant,  $\nu$  in the equation (3.2) is described as:

$$\nu = \nu_v + \nu_t, \quad (3.3)$$

where  $\nu_v$  is the kinematic viscosity coefficient,  $\nu_t$  the eddy viscosity coefficient.

The behavior of free surface is tracked by Volume of Fluid (VOF) method. The advective equation of fluid volume is represented as:

$$\frac{\partial F}{\partial t} + u_j \frac{\partial F}{\partial x_j} = 0, \quad (3.4)$$

where,  $F$  is the ratio of existing fluid volume in the cell.

In the finite difference equations derived from the basic equations described above, the time and advection terms are approximated by the forward and the third-order upwind finite difference, respectively, while the other terms the centered difference. We adopt the Semi-Implicit Method for Pressure-Linked Equation (SIMPLE) method for time integration scheme.

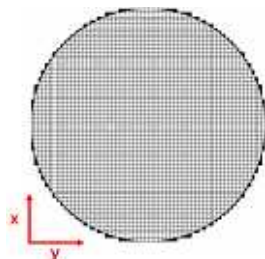


**Fig.13** Calculating cell in horizontal section

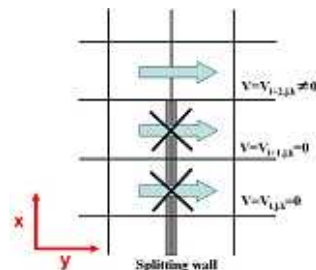


**Fig.14** Numerical modeling of splitting wall

The analytical condition is listed in **Table 2**. Based on the coordinate system shown in **Fig.2**, we divide the

analyzed region into 64 cells with 8 mm width in x and y directions and 60 cells with 5 mm height in z direction. **Fig.13** shows the computation cells used in this simulation. Total 200,898 cells are used. The splitting wall is modeled as the boundary which the fluid does not go through as shown in **Fig.14**. Note that the splitting wall is assumed to have no thickness.

Table 2 Numerical condition

input motion	sinusoidal motion	observed ground motion
time step $t$	0.005s	0.001s
B.C. of fluid velocity	free slip	
interval in x direction	8mm (64 cells in x direction)	
interval in y direction	8mm (64 cells in y direction)	
interval in z direction	8mm (60 cells in z direction)	

The horizontal accelerations, which are sinusoidal motion whose amplitude is 1mm and observed on the ground surface during the 2003 Tokachi-oki earthquake, is input to  $G_i$  in equation (3.2). The time step is set to 0.005 seconds for the sinusoidal motion and 0.001 seconds for the observed ground motion.

### 3.2 Comparison of responses between numerical and experimental results

**Fig. 15** and **Figs. 16(a)-(e)** show the comparisons of the sloshing height response curves between numerical and experimental results in the cases #00, #07, #06, #11, #12 and #16. In these figures, solid line (marked by  $\circ$ ) shows the numerical result and dash line (marked by  $\diamond$ ) the experimental one. Comparison of the sloshing height response between numerical and experimental results in the case #00 (no splitting wall case, OR=100%) is shown in **Fig. 15**. Both results have two peaks whose values are almost identical. This indicates that the numerical results can simulate the experiment with good accuracy in the case #00. In the cases with splitting wall shown in **Fig. 16**, the natural frequency at half tank mode in numerical results agrees well with that in experimental results, while some of the peak values in experiment results exceed that in numerical results a little. **Fig.16 (e)** shows the comparison of sloshing height response in the case #16 which is the best case in the model experiments. Almost same sloshing height response curves are obtained in wide frequency range, while the numerical results are a little smaller than experimental results. The numerical results also indicate that the splitting wall in the case #16 shows the good performance.

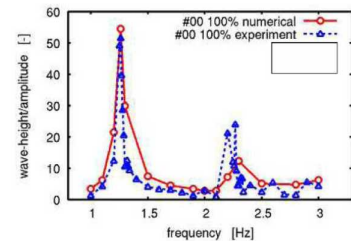


**Fig.15** Comparison of sloshing height response curves in the case #00 between numerical(  $\circ$  ) and experimental(  $\diamond$  )

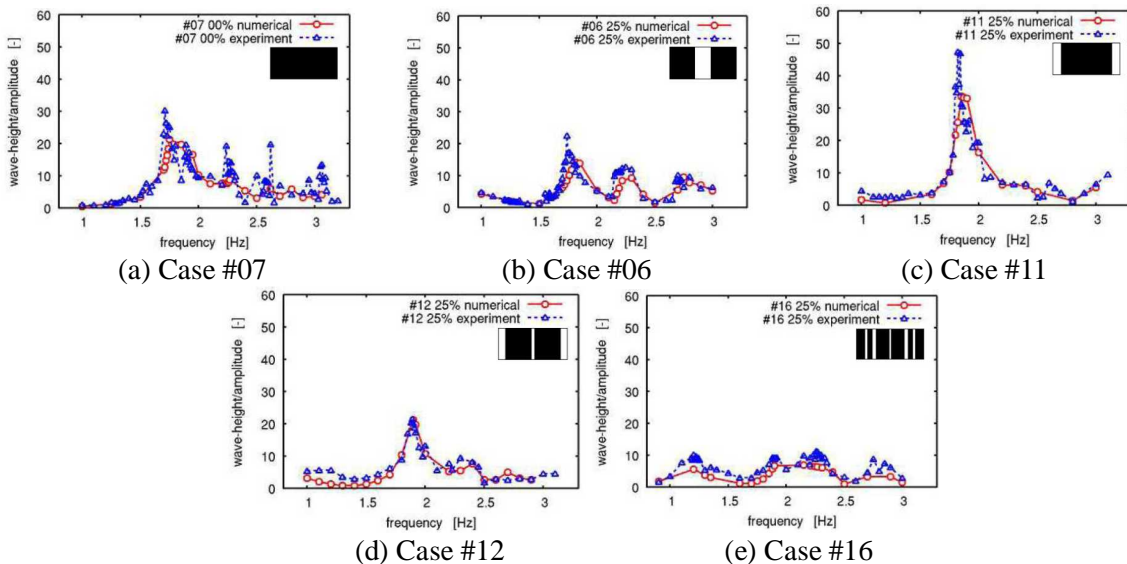


**Fig.16** Comparison of sloshing height response curves between numerical(  $\circ$  ) and experimental(  $\diamond$  ) results

Fig.17 shows the comparison of the fluid load response curves between numerical and experimental results in the cases #07, #06, #11, #12 and #16. The meanings of lines and marks in the figure are same as these in Fig. 16. Similar fluid load response curves are also obtained in wide frequency range. This indicates that the numerical method can accurately simulate the sloshing behavior of the cylindrical tanks with splitting wall.

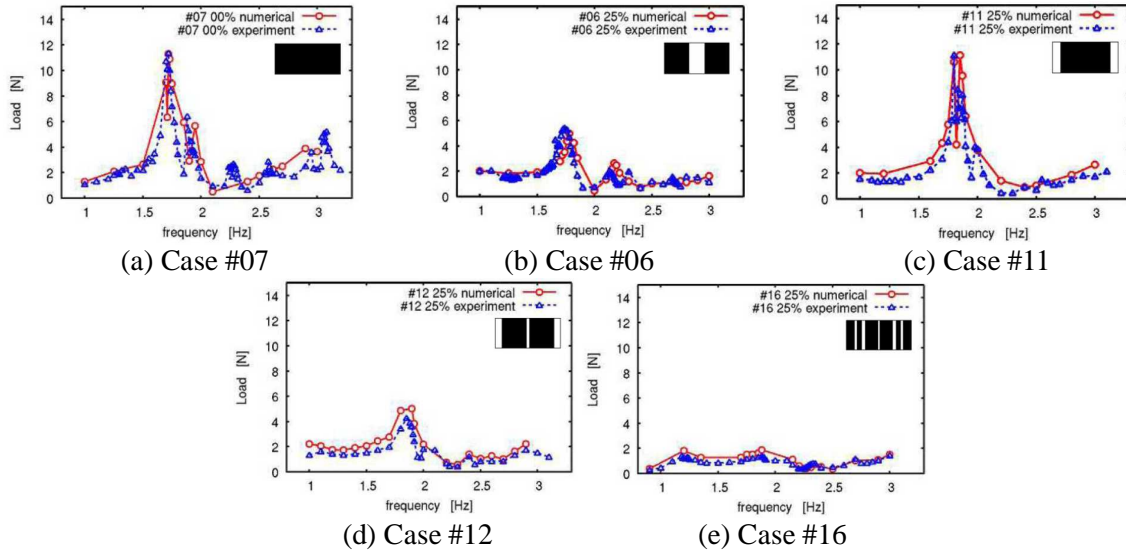


Fig. 17 Comparison of the fluid load response curves between numerical( ) and experimental( ) results

### 3.3 Simulation using the observed earthquake ground motion

The sloshing response is calculated against the EW component of observed ground motion during the 2003 Tokachi-oki earthquake at Tomakomai observation station (HKD129) in Hokkaido prefecture, Japan, which is operated by National Research Institute for Earth science and Disaster prevention (NIED). Note that the record is scaled in time domain for turning the predominant frequency to the natural frequency of first sloshing mode. Fig.18 shows the input motion in the model scale. Fig.19 shows time history of sloshing response height in the case #00, which is no splitting wall case. In this case, the peak value of sloshing height is about 24 mm when the time is about 10 sec. Fig.20 shows sloshing response in the case #07, whose peak value is reduced about 25%. The peak value of sloshing height in the case #16 is about one third of that in the case #00 as shown in Fig.21. It can be concluded that the splitting wall in the case #16 is also effective against earthquake ground motions.

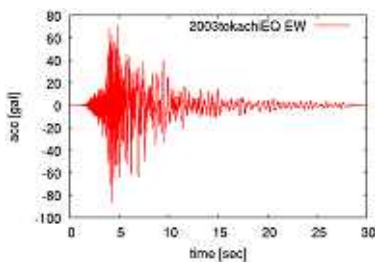


Fig.18 Input motion

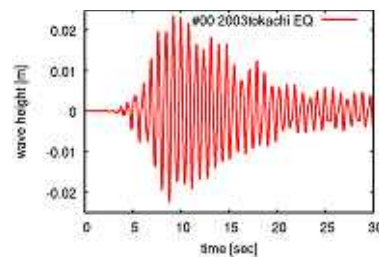


Fig.19 Time history of sloshing height in case #00

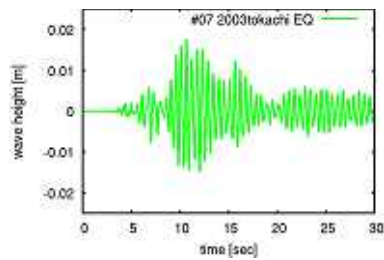


Fig.20 Time history of sloshing height in case #07

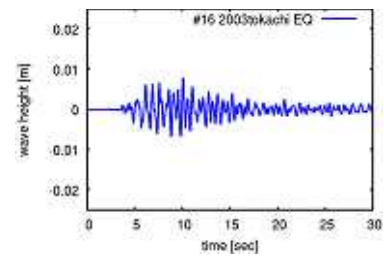


Fig.21 Time history of sloshing height in case #16

#### 4.CONCLUSION

We develop a splitting wall as a new sloshing reduction device for cylindrical tanks. Model experiments and numerical simulations are performed to examine the effect of the device. The results obtained by this study are shown as follows.

1. The splitting wall installed in tanks reduces sloshing height, especially for first natural mode, while it generates new other mode on frequency response, which is called “half tank mode”.
2. We propose the effective slit layout of splitting wall based on the model experiments. In the case #16, sloshing height can be largely reduced in wide frequency range including the new mode.
3. The numerical results agree well with the experimental ones in all cases. It indicates that the numerical method used can simulate sloshing motion in cylindrical tanks with the splitting wall.
4. We perform numerical simulation using an observed earthquake ground motion. It is concluded that the splitting wall in the case #16 can reduce sloshing height a lot against not only sinusoidal motion but also earthquake ground motions.

#### Acknowledgement

We thank Miyasaka Corporation a lot for producing the experimental model. We also thank NIED (National Research Institute for Earth science and Disaster prevention) for providing the earthquake ground motion recorded.

#### REFERENCES

- Shinsaku Z. (2005). “Fudge earthquake and large-scale structure” (in Japanese)
- Kazuki K., Ken H., Takashi F., Yasushi I., Shunichi A. (2005). “Damaging Long-period Ground Motions from the 2003  $M_w$  8.3 Tokachi-oki, Japan Earthquake”. *Seismological Research Letters*, 74:1, 67-73
- J.R.Cho., and S.Y.Lee. (2003). “Dynamic analysis of baffled fuel-storage tanks using the ALE finite element method”. *International Journal for Numerical Methods in Fluids*, 41, 185-208
- Kanae S., Kenji N. (1954). “On the Vibration of an Elevated Water-Tank-I”. *Technical Report of The Osaka University*, Vol4, No.117, pp.247-264
- Hirt, C.W., and Nichols, B.D. (1981). “Volume of fluid (VOF) method for the dynamics of free boundaries”. *Journal of computational physics*, 39, 201-225
- Patankar, S.V., and Spalding, D.B. (1972). “A calculation procedure for heat, mass and momentum transfer in three-dimension parabolic”. *Journal of heat mass transfer*, 15, 1787